

150 million years of sustained increase in pterosaur flight efficiency

Chris Venditti^{1*}, Joanna Baker¹, Michael J. Benton², Andrew Meade¹ and Stuart
Humphries^{3*}

Affiliations:

¹School of Biological Sciences, University of Reading, Reading RG6 6BX, United
Kingdom.

²School of Earth Sciences, University of Bristol, Life Sciences Building, Tyndall
Avenue, Bristol BS8 1TQ, United Kingdom.

³School of Life Sciences, University of Lincoln, Joseph Banks Laboratories, Green
Lane, Lincoln LN6 7DL, United Kingdom.

*Correspondence to c.d.venditti@reading.ac.uk and shumphries@lincoln.ac.uk.

Summary

The long-term accumulation of biodiversity has been punctuated by remarkable evolutionary transitions that allowed organisms to exploit new ecological opportunities. Mesozoic flying reptiles – the pterosaurs – which dominated the skies for over 150 million years (myr) were the product of one such transition. The ancestors of pterosaurs were small and likely bipedal early archosaurs¹, which were certainly well adapted to terrestrial locomotion. Pterosaurs diverged from dinosaur ancestors in the Early Triassic (~245 myr ago, Ma), and yet their first fossils come 25 myr later, in the Late Triassic. Thus, in the absence of proto-pterosaur fossils, it is difficult to study how flight first evolved in this group. Our aim here is to study the evolutionary

dynamics of pterosaurs' adaptation to a new locomotory medium. The earliest known pterosaurs took flight and subsequently appear to have become capable and efficient flyers. However, it seems clear that transitioning between forms of locomotion^{2,3} - from terrestrial to volant – challenged early pterosaurs by imposing a steep energetic hill to climb, thus requiring flight to provide some offsetting fitness benefits. Using novel phylogenetic statistical methods and biophysical models combined with information from the fossil record, we detect an evolutionary signal of natural selection acting to increase flight efficiency over millions of years. Our results show that there was still significant room for improvement in terms of efficiency after the appearance of flight. However, in the Azdarchoidea⁴, a clade exhibiting gigantism, we test the hypothesis that there was a decreased reliance on flight⁵⁻⁷ and find evidence for reduced selection on flight efficiency in this clade. By combining biophysical models and phylogenetic statistical methods with the fossil record, we offer a blueprint to study functional and energetic changes through geological time objectively at a far more nuanced level than has ever before been possible.

In order to determine how pterosaurs' propensity for flight changed during their evolutionary history, we calculated two indices of flight performance using a biophysical model of powered and gliding flight⁸⁻¹⁰. Firstly, we used an efficiency of flight index (kg m J^{-1}), that is the inverse of the cost of transport¹⁰, CoT^{-1} (see Methods and Table S1 for the flight model parameterization). The CoT ($\text{J kg}^{-1}\text{m}^{-1}$) is the metabolic energy required to move a unit mass a unit distance at the least energetically expensive travel speed. Secondly, we calculated a sinking rate¹⁰, V_z (m

s⁻¹, see Methods) valid for gliding. A low sinking rate allows for longer travel distances per glide, but also for climbing in updrafts where sinking rate must be lower than the rate at which air rises from the ground. Both CoT^{-1} and V_z were calculated using published estimates of mass^{11,12}, wingspan¹³, wing area^{11,12}, and projected frontal area¹². The dataset we use in this paper has mass and wing area estimates for 16 species of pterosaur¹¹ (Table S2, Methods). Although an alternative dataset of mass and wing area estimates is available for 12 species¹², the two datasets cannot be combined owing to considerable differences in the approaches of each paper to body mass estimation (and the fact that the two datasets overlap). However, our results are qualitatively the same using mass and wing area estimates from each of the two datasets in isolation, and so here we only report the results from one dataset¹¹. We use published frontal areas¹² and wingspans¹³ (see Methods for details).

Studying the changes in CoT^{-1} and V_z through time can inform us about how evolutionary changes such as natural selection have acted on flight performance throughout the course of pterosaur evolution. The lack of proto-pterosaurs in the fossil record means that it is currently impossible to be sure how the pterosaurs initially overcame the energetic hill necessary to achieve flight. Our aim is to study the evolutionary dynamics of pterosaurs' adaptation to a new locomotory medium. The earliest known pterosaur fossils indicate they were able to fly¹⁴. If during their 150 myr of evolution their flight performance and efficiency did not improve or decrease we would expect to see no trend in CoT^{-1} and V_z over time (Figure 1a). We might however expect that after the start of a transition involving a change in the defining medium of locomotion (i.e. from terrestrial to volant), species would be relatively energetically inefficient at moving in the new environment. Thus, over time

they would become more efficient. In this case, we would expect flight efficiency (CoT^{-1}) to increase through time and sinking rate (V_z) to decrease (Figure 1b). We would expect the opposite (a decrease in CoT^{-1} and an increase in V_z over time) if flight performance reduced over time (Figure 1c).

In order to study the evolution of flight (including calculation of the flight performance indices), it is necessary to account for shared ancestry owing to phylogeny. Several phylogenetic trees for pterosaurs exist in the literature ^{e.g. 1,15,16}, but none of these provides well-justified estimates of the uncertainty among species relationships and divergence dates. To account for phylogenetic and temporal uncertainty in our analyses we constructed a Bayesian dated posterior sample of phylogenetic trees for 128 pterosaurs using published character state data¹⁵ (Figure 2, Supplementary Data 1, and see Methods).

Wingspan is strongly associated with pterosaur morphologies. We find wingspan explained 97% (range of the posterior distribution, 95–98%) of the variation in mass, 97% (96–98%) of the variation in wing area, and 75% (71–87%) of the variation in frontal area. Then using a phylogenetic prediction method¹⁸ we derived a posterior distribution of imputed masses, projected frontal area and wing area for a further 59 species of pterosaurs based on the results of the phylogenetic regression analyses and our phylogenetic tree (Table S2). Our use of Bayesian phylogenetic methods means we integrate our analyses over all phylogenetic (topology and divergence dates) and model uncertainties. Thus, based on our imputations, we calculated a posterior distribution of 1000 CoT^{-1} and 1000 V_z estimates for use in our analyses of flight performance through time (see Methods). These imputations are robust to jack-knife re-sampling (see Extended Data Figure 1). Our final set of analyses used information from 75 species, including the

uncertainty from imputed values that span the majority of the phylogenetic diversity of all known pterosaurs (Figure 2a).

While CoT^{-1} is an efficiency index related to the amount of energy needed to travel a given distance, independently of how long it takes, we do expect it to correlate with mass¹⁹. It is energetically cheaper for a large animal to move a given mass over a particular distance than for a small animal to travel the same distance²⁰ (Figure 2b). Sinking rate is similarly affected by mass (Figure 2c) and reflects the relationships we know for birds and bats (Extended Data Figure 2, Supplementary Information).

This relationship with mass means that we need to simultaneously consider mass and its evolutionary association with flight performance in our analyses of flight efficiency and sinking rate through time. With this in mind, pterosaurs have been reported to conform with the well-known Cope's rule¹³ – a phenomenon where species increase in size through geological time. The most compelling evidence for this is derived from analyses reporting an increase in wingspan from ~150 Ma to the end of the Cretaceous (~66 Ma) coincident with the origin of birds (Avialae)¹³. However, such a trend could emerge as a consequence of increased flight efficiency rather than increase in body size *per se*. Animals with a larger wingspan for their mass are likely to be more efficient flyers⁹. We find using a phylogenetic regression model that accounts for the uncertainty in our inferred tree and our estimates of species masses, frontal area and wing area (see Methods), that pterosaur size did increase significantly through time. In addition, a model that allows the rate of mass increase through time to differ before and after the origin of the birds fits significantly better than a model without such an inflection. In line with earlier conclusions¹³, we find that there is no significant increase in size until ~150 Ma ($p_x = 0.59$). From that

point the average pterosaur grew significantly from 0.60 kg to 6.05 kg (proportion of the posterior distribution that crosses zero, $p_x = 0.02$), a ~10-fold increase in size, over 65 million years.

Turning now to flight performance, there is a growing body of evidence indicating that the Azhdarchoidea had strong terrestrial affinities^{5-7,21} (cf. ²²). Here the Azhdarchoidea are considered to comprise the common ancestor and all descendants of *Tapejara*, *Quetzalcoatlus*, and *Dsungaripterus*¹ (posterior nodal support = 0.83 in our phylogeny). Evidence suggests that azhdarchoid pterosaurs had relatively inflexible necks⁷, left tracks indicating terrestrial proficiency⁵, and possessed other adaptations associated with ground-dwelling generalist foraging (reviewed^{6,7}). *Dsungaripterids* (the most basal azhdarchoids in our phylogeny, Figure 2) are reported to have been wading foragers^{14,21} feeding on hard-shelled organisms at water margins²³. Given the terrestrial tendencies in the Azhdarchoidea compared to what we know about other pterosaurs, we might expect diminished reliance on flight, leading to the expectation that they might have differed from other pterosaurs in the selection pressures for adaptations associated with flight and locomotion. Thus, in our analyses we test whether the evolution of flight performance through time in the Azhdarchoidea is distinct from other pterosaur species.

Applying phylogenetic regression to flight efficiency through time we find that, even after accounting for mass, efficiency increased significantly ($p_x = 0.00$, Figure 3a–c) in non-azdarchoid pterosaurs. However, in contrast to our finding for mass, there is no significant effect associated with the arrival of birds ($p_x = 0.47$). Early pterosaurs (<200 Ma) had an average efficiency of 0.29 kg m J⁻¹ but by 70 Ma they were greater than 50% more efficient (CoT⁻¹ = 0.51 kg m J⁻¹). Congruently we find that sinking rate (after accounting for mass) for non-azdarchoid pterosaurs reduced

from 0.80 m s^{-1} to 0.50 m s^{-1} over the course of the 150 myr of their evolutionary history (Figure 3d–f). In contrast, azdarchoids exhibited no change in efficiency or sinking rate from origin to extinction.

Our results show that, save for azdarchoids, following their transition to volant locomotion, the pterosaurs exhibited a sustained increase in flight efficiency over 150 myr until their extinction. To achieve this, natural selection acted to decouple the evolution of body size and wingspan (Figure 3g–i) to sculpt these enigmatic creatures from what might have been inefficient flyers that took to the air for only short spells, to creatures that could fly long distances over extended periods. At their origin, some ~147 Ma, 85 myr after the origin of crown pterosaurs, azdarchoids had a slightly lower flight efficiency and higher sinking rates compared with their contemporaries – and showed no temporal trends in either trait until their eventual extinction (Figure 3a–f). This reduced pattern of flight efficiency is also borne out in analyses of gross morphology - azdarchoids arose with short wings for their size, and maintained this condition until their final demise.

Our approach demonstrates the power of combining biophysical models and phylogenetic statistical methods with the fossil record to understand the evolution of flight in pterosaurs. In doing so we offer a blueprint to study functional and energetic changes objectively through geological time at a far more nuanced level than has ever before been possible.

References

1 Andres, B., Clark, J. & Xu, X. The earliest pterodactyloid and the origin of the group. *Curr. Biol.* **24**, 1011-1016, doi:<http://dx.doi.org/10.1016/j.cub.2014.03.030> (2014).

- 173 2 Williams, T. M. The evolution of cost efficient swimming in marine mammals:
174 Limits to energetic optimization. *Philos T R Soc B* **354**, 193-201 (1999).
- 175 3 Alexander, R. M. Bioenergetics. One price to run, swim or fly? *Nature* **397**,
176 651-653, doi:10.1038/17687 (1999).
- 177 4 Naish, D. & Witton, M. P. Neck biomechanics indicate that giant
178 Transylvanian azhdarchid pterosaurs were short-necked arch predators. *PeerJ* **5**,
179 e2908 (2017).
- 180 5 Hwang, K.-G., Huh, M., Lockley, M. G., Unwin, D. M. & Wright, J. L. New
181 pterosaur tracks (Pteraichnidae) from the Late Cretaceous Uhangri formation,
182 southwestern Korea. *Geol Mag* **139**, 421-435 (2002).
- 183 6 Witton, M. P. & Naish, D. Azhdarchid pterosaurs: Water-trawling pelican
184 mimics or “terrestrial stalkers”? *Acta Palaeontol. Pol.* **60**, 651-660, 610 (2013).
- 185 7 Witton, M. P. & Naish, D. A reappraisal of azhdarchid pterosaur functional
186 morphology and paleoecology. *PLoS ONE* **3**, e2271 (2008).
- 187 8 Humphries, S., Bonser, R. H., Witton, M. P. & Martill, D. M. Did pterosaurs
188 feed by skimming? Physical modelling and anatomical evaluation of an unusual
189 feeding method. *PLoS Biol.* **5**, e204 (2007).
- 190 9 Pennycuick, C. J. *Modelling the flying bird*. Vol. 5 (Elsevier, 2008).
- 191 10 Taylor, G. & Thomas, A. *Evolutionary biomechanics: Selection, phylogeny,*
192 *and constraint*. (Oxford University Press, 2014).
- 193 11 Witton, M. P. A new approach to determining pterosaur body mass and its
194 implications for pterosaur flight. *Zitteliana* **28**, 143-158 (2008).

- 195 12 Henderson, D. M. Pterosaur body mass estimates from three-dimensional
196 mathematical slicing. *J Vert Paleontol* **30**, 768-785,
197 doi:10.1080/02724631003758334 (2010).
- 198 13 Benson, R. B. J., Frigot, R. A., Goswami, A., Andres, B. & Butler, R. J.
199 Competition and constraint drove Cope's rule in the evolution of giant flying reptiles.
200 *Nat Commun* **5**, doi:10.1038/ncomms4567 (2014).
- 201 14 Witton, M. P. *Pterosaurs: Natural history, evolution, anatomy*. (Princeton
202 University Press, 2013).
- 203 15 Longrich, N. R., Martill, D. M. & Andres, B. Late Maastrichtian pterosaurs from
204 North Africa and mass extinction of Pterosauria at the Cretaceous-Paleogene
205 boundary. *PLoS Biol.* **16**, e2001663 (2018).
- 206 16 Andres, B. & Myers, T. S. Lone star pterosaurs. *Earth Env Sci T R Soc Edinb*
207 **103**, 383-398, doi:doi:10.1017/S1755691013000303 (2012).
- 208 17 Schliep, K. P. Phangorn: Phylogenetic analysis in R. *Bioinformatics* **27**, 592-
209 593 (2011).
- 210 18 Organ, C. L., Shedlock, A. M., Meade, A., Pagel, M. & Edwards, S. V. Origin
211 of avian genome size and structure in non-avian dinosaurs. *Nature* **446**, 180-184,
212 doi:10.1038/nature05621 (2007).
- 213 19 Bale, R., Hao, M., Bhalla, A. P. S. & Patankar, N. A. Energy efficiency and
214 allometry of movement of swimming and flying animals. *Proc Natl Acad Sci U S A*
215 **111**, 7517-7521, doi:10.1073/pnas.1310544111 (2014).
- 216 20 Alexander, R. M. Models and the scaling of energy costs for locomotion. *J*
217 *Exp Biol* **208**, 1645-1652, doi:10.1242/jeb.01484 (2005).

- 218 21 Unwin, D. M. *The pterosaurs from deep time*. (Pi Press, New York, 2005).
- 219 22 Averianov, A. Reconstruction of the neck of *Azhdarcho lancicollis* and lifestyle
220 of azhdarchids (pterosauria, azhdarchidae). *Paleontol J* **47**, 203-209 (2013).
- 221 23 Bestwick, J., Unwin, D. M., Butler, R. J., Henderson, D. M. & Purnell, M. A.
222 Pterosaur dietary hypotheses: A review of ideas and approaches. *Biol Rev* **93**, 2021-
223 2048 (2018).

224 **Figure Legends**

225 **Figure 1: Hypothesised scenarios of the evolutionary trajectory of flight**
226 **performance metrics through time.** a) No relationship between flight performance
227 metrics and time would indicate no directional change in flight ability through time. b)
228 An increase in efficiency through time and a reduction in sinking rate would
229 demonstrate a general tendency for selection favouring increased flight performance
230 as the pterosaurs radiated. c) A decrease in efficiency and an increase in sinking
231 rate would imply a reduction in flight performance through time. The branches of the
232 phylogenetic trees are coloured by hypothesised magnitudes of efficiency (green)
233 and sinking rate (blue).

234

235 **Figure 2: Pterosaur phylogeny and the relationship of flight performance**
236 **metrics with mass.** a) Density diagram ¹⁷ showing the uncertainty in our
237 phylogenetic reconstruction for pterosaurs (n=128, see Methods for details).
238 Superimposed is the maximum clade credibility tree and triangle points indicate
239 species for which we have published data on mass, wing area, frontal area, and
240 wingspan. Circle points indicate species for which we have wingspan only. Red
241 denotes azdarchoids. b) The relationship between flight efficiency and mass (n=75),

with our mean phylogenetic imputations plotted with standard deviations shown by the green ellipses. c) The relationship between sinking rate and mass (n=75), with our mean phylogenetic imputations plotted with standard deviations shown by the blue ellipses. Silhouette of Eudimorphodon is taken from phylopic.org and is available for reuse under the Public Domain Dedication 1.0 license (<https://creativecommons.org/publicdomain/zero/1.0/>), credit to Steven Traver.

Figure 3: Flight performance through time. Summary plots for each of our three main traits of interest (efficiency, a–c; sinking rate, d–f; wingspan, g–i). A phylogeny of the species included in each analysis (a, d, g) is shown with branches shaded by reconstructed trait values; Azdarchoidea is highlighted in red. Trait data are shown plotted against time (b, e, h) where all species with imputed values are represented by circles – excepting wingspan data which is all from published sources. Points are coloured by species' body mass and azdarchoid species are outlined in red. The posterior distribution of model predictions for each trait against time (c, f, i) shows how these traits evolved during pterosaur history. These relationships demonstrate that – after accounting for size – pterosaurs continually increased their efficiency (c) and wingspan (i) whilst there was a continual reduction in sinking rate (f) through time (grey lines, median in black). This applies to all pterosaurs except azhdarchoids (pink lines, median in red) which show no significant trends – although they do have relatively short wings for their mass (i). Silhouette of Eudimorphodon (black) is taken from phylopic.org and is available for reuse under the Public Domain Dedication 1.0 license (<https://creativecommons.org/publicdomain/zero/1.0/>), credit to Steven Traver. Silhouette representing Azdarchoidea (red) is taken from phylopic.org and is available for reuse under the Creative Commons Attribution 3.0 Unported license (<https://creativecommons.org/publicdomain/zero/1.0/>), credit to Darren Naish (vectorized by T. Michael Keesey).

269

270

271

272 **Methods**

273 *Phylogenetic Inference*

274 All morphological data were obtained from a published phylogenetic character
275 matrix¹⁵. However, we retained only discrete morphological characters, excluding the
276 continuously varying characters, and treating all ordered characters as unordered,
277 resulting in a total of 220 discrete morphological characters coded for 128 pterosaur
278 species.

279 We constructed a posterior sample of time-calibrated phylogenetic trees for
280 pterosaurs using the birth-death serial-sampling model^{24,25} as implemented in
281 BEAST v2.4²⁶ allowing for simultaneous estimation of both the topology and
282 divergence times. For each species, we tip-dated using the midpoint of the
283 stratigraphic age representing the first appearance of each species using published
284 time intervals^{1,13,15}. The origin of the birth-death process was estimated from a
285 uniform prior distribution ranging from the age of the youngest species in the tree
286 (*Eudimorphodon rosenfeldi*) up to an arbitrary upper limit of 350 Ma.

287 Owing to the lack of information about speciation and extinction rates in the
288 pterosaur literature we took a conservative approach by placing a wide uninformative
289 prior distribution (uniform ranging between 0 and infinity) on both the effective
290 reproductive number (the birth-death ratio) and the “become uninfected rate” (total
291 death rate). Similarly, we placed an uninformative uniform prior between 0 and 1 on
292 the sampling proportion. Together, these parameters enable direct estimation of
293 birth-death rates throughout the phylogenetic tree²⁴.

294 We modelled rate heterogeneity across lineages using an uncorrelated
295 relaxed morphological clock²⁷. We placed an exponential prior (mean = 1) on the
296 mean of the lognormal distribution from which the branch-wise clock rates are drawn,

and a gamma prior ($\alpha = 0.5396$, $\beta = 0.3819$) on the standard deviation. Characters were partitioned on the basis of the number of discrete states, and we applied Lewis' Markov k (Mk) model of morphological character evolution²⁸ across all partitions, estimating a shared gamma shape parameter (Γ_4)²⁹ using an exponential prior distribution with mean = 1.

The MCMC chain was run for one billion iterations, sampling every 100,000 iterations after convergence. To produce the posterior sample of 1,000 phylogenetic trees used in the main analyses, we randomly sampled 1,000 iterations from this chain, ensuring that all parameters had an effective sample size of >500, calculated using Tracer v1.6³⁰. We ensured that all parameters that were estimated using a uniform uninformative prior (origin, effective reproductive number, become uninfected rate, and the sampling rate) returned a posterior distribution of estimates that differed from the prior. The analysis was repeated multiple times to ensure convergence was reached. All chains were inspected visually using Tracer v1.6³⁰.

The full sample is visualized in Figure 2a as a density tree produced in R³¹ using functions available in the package phangorn¹⁷, and is available to download in nexus format as Supplementary Data 1 of this article.

Imputation of pterosaur measurements

To calculate our efficiency index (see below) we required mass, frontal area and wing area for adult pterosaur species. Estimates for mass and wing area are available for N=16 species from Witton¹¹ and N=12 species from Henderson¹² (see Table S2). For frontal area values are taken from Henderson¹² (N = 12, though see below). Independently for each of the two datasets, we used the phylogenetic method outlined in¹⁸ to impute a posterior sample of 1000 estimates of mass, frontal

area and wing area for a total of $N = 75$ species. We obtained wingspans for additional species from¹³ (a list of species used is found in Table S2) and used each morphological trait's relationship with wingspan (i.e. a phylogenetic regression of each trait against wingspan) to impute species-specific values. As a part of this procedure, we also imputed frontal area for the $N=7$ species in the Witton¹¹ dataset which did not have data in Henderson¹² (see Table S2).

Flight energetics model

Animal powered flight energetics, while perhaps kinematically different for bats, birds and pterosaurs, are still ultimately constrained by physics. It has previously been demonstrated that it is possible to infer flight performance of pterosaurs using biophysical models of flight in combination with metabolic scaling estimates from birds⁸. Here we used an actuator-disc based model owing to the pedigree of this approach and because more complex wake dynamics models and computational approaches are particularly difficult to parameterize, requiring a number of kinematic parameters such as wingbeat frequency that are impossible to infer from fossil material. We used a modified version of Pennycuick's Flight model (v1.25)⁹ that we developed from earlier work⁸ and implemented in Matlab^{®32}, and which includes published parasite power estimates³³. Flight performance is estimated based on morphological measurements such as body mass, wingspan and wing area (Table S1) and the model produces a U-shaped power-to-airspeed relationship, from which a minimum power speed (V_{mp}) can be calculated. This V_{mp} is the least energetically expensive flight speed and so provides a useful proxy for efficiency¹⁰ when incorporated into the CoT.

We used the model to estimate the metabolic and mechanical power required for powered (flapping) flight given information on a minimal set of morphological

traits and estimates of physiology, as well as aerodynamic constants (Table S1). The intersection of the power curve with an animal's available metabolic power (P_{BMR} , calculated from mass and estimated basal metabolic rate, BMR) allows us to characterise flight ability^{9,34}. Consistent with current thought^{35,36}, and in line with previous studies⁸, we assume that pterosaurs had a BMR similar to that of birds.

Estimation of energetic efficiency

A number of energetic efficiency measures exist¹⁰ but one useful proxy is the inverse of the mass specific Cost of Transport (CoT, the energy required to move a unit mass a unit distance, independent of the time taken to do so). We estimate CoT as $P_{\text{BMR}}/(V \times M)$ where V is the least energetically expensive travel speed (i.e. V_{mp}) and other parameters are as in Table S1.

For species with available data (Table S2) we produced a single estimate of CoT^{-1} using the inverse of the above formula. For each of the species for which we imputed mass, frontal area and wing area (Table S2 and above), we use the full sample of our imputed values to produce a posterior sample of 1000 estimates of CoT^{-1} .

As formulated, CoT accounts for mass. However, as energy efficiency appears to increase with body size^{19,20} we included size in our regression model of CoT^{-1} through time (main text and see below) to account for this.

Estimation of sinking rate

Sinking rate while gliding (V_z) was calculated as $D \times V_{\text{mp}} / M \times g$ (where D is the total aerodynamic drag resulting from the addition of the induced, parasite and profile drags) and assuming a linear wingspan reduction (see³⁴).

370 *Phylogenetic regression models testing temporal trends in mass and efficiency*
371 To test the evolutionary trajectories of pterosaur mass and measures of flight
372 efficiency through time we use phylogenetic generalized least squares^{37,38} multiple
373 regression models in a Bayesian framework. We assessed the significance of
374 regression parameters using the proportion of the posterior distribution that crosses
375 zero, p_x , where we consider $p_x < 0.05$ as significant. In addition to the 16 species for
376 which we have single estimates of body mass, V_z and CoT^{-1} from¹¹ (or $N = 12$
377 from¹²), in all our models we include the full set of posterior estimates of both body
378 mass and CoT^{-1} for all species for which the data are imputed (Table S2). These
379 values are sampled in proportion to their probability during the running of the MCMC
380 chain. This allows us to incorporate information about the variance of our
381 imputations, avoiding problems associated with summarizing the posterior
382 distribution into a single point estimate.
383

Methods References

- 24 Stadler, T. Sampling-through-time in birth–death trees. *J. Theor. Biol.* **267**, 396–404, doi:10.1016/j.jtbi.2010.09.010 (2010).
- 25 Stadler, T., Kühnert, D., Bonhoeffer, S. & Drummond, A. J. Birth–death skyline plot reveals temporal changes of epidemic spread in HIV and hepatitis C virus (HCV). *Proc Natl Acad Sci U S A* **110**, 228–233, doi:10.1073/pnas.1207965110 (2013).
- 26 Bouckaert, R. *et al.* BEAST 2: A software platform for Bayesian evolutionary analysis. *PLoS Comp. Biol.* **10**, e1003537, doi:10.1371/journal.pcbi.1003537 (2014).
- 27 Drummond, A. J., Ho, S. Y. W., Phillips, M. J. & Rambaut, A. Relaxed phylogenetics and dating with confidence. *PLoS Biol.* **4**, e88, doi:10.1371/journal.pbio.0040088 (2006).
- 28 Lewis, P. O. A likelihood approach to estimating phylogeny from discrete morphological character data. *Syst. Biol.* **50**, 913–925, doi:10.1080/106351501753462876 (2001).
- 29 Yang, Z. Maximum likelihood phylogenetic estimation from DNA sequences with variable rates over sites: Approximate methods. *J. Mol. Evol.* **39**, 306–314 (1994).
- 30 Tracer v. 1. 6. 2014 (2015).
- 31 R: A language and environment for statistical computing (R Foundation for Statistical Computing., 2016).
- 32 The Mathworks inc. (Natick, MA, 2017).

- 406 33 Ward, C. V. Interpreting the posture and locomotion of *Australopithecus*
407 *afarensis*: Where do we stand? *Am. J. Phys. Anthropol.* **119**, 185-215 (2002).
- 408 34 Pennycuik, C. J. *Bird flight performance*. (Oxford University Press, USA,
409 1989).
- 410 35 Clarke, A. Dinosaur energetics: Setting the bounds on feasible physiologies
411 and ecologies. *Am Nat* **182**, 283-297, doi:10.1086/671259 (2013).
- 412 36 Pontzer, H., Allen, V. & Hutchinson, J. R. Biomechanics of running indicates
413 endothermy in bipedal dinosaurs. *PLoS ONE* **4**, e7783,
414 doi:10.1371/journal.pone.0007783 (2009).
- 415 37 Pagel, M. Inferring evolutionary processes from phylogenies. *Zool Scr* **26**,
416 331-348, doi:10.1111/j.1463-6409.1997.tb00423.x (1997).
- 417 38 Freckleton, R. P., Harvey, P. H. & Pagel, M. Phylogenetic analysis and
418 comparative data: A test and review of evidence. *Am Nat* **160**, 712-726,
419 doi:10.1086/343873 (2002).
- 420

Acknowledgements

We thank Ciara O'Donovan, Mark Pagel, Graeme Ruxton, and Manabu Sakamoto for helpful discussions during the course of this research. JB is funded by the Leverhulme Trust (ECF-017-22). CV was funded by a Leverhulme Trust Research Project Grant (RPG-2017-071).

Author Contributions

C.V and S.H. conceived the study. C.V., J.B., M.B., and S.H. collected the data. C.V., J.B., A.M., and S.H. conducted the phylogenetic and biophysical analyses. C.V., J.B., A.M., M.B. and S.H. interpreted the results and wrote the paper.

Author Information

¹School of Biological Sciences, University of Reading, Reading RG6 6BX, United Kingdom.

²School of Earth Sciences, University of Bristol, Life Sciences Building, Tyndall Avenue, Bristol BS8 1TQ, United Kingdom.

³School of Life Sciences, University of Lincoln, Joseph Banks Laboratories, Green Lane, Lincoln LN6 7DL, United Kingdom.

*Correspondence to c.d.venditti@reading.ac.uk and shumphries@lincoln.ac.uk.

The authors declare no competing financial interests.

Data Availability Statement

The phylogeny we generated in this study (presented in Figure 2a) is included as Supplementary Information (Supplementary Data File 1) with this article. No other data was generated or analysed during the current study. All data used are available from published sources and are cited in the main text where appropriate.

Software and Code

All analyses in this research were conducted using readily available, published programs and are cited in the text. Version numbers of the programs we used are as follows: Tracer v1.6. (2015), MATLAB v9.2 (2017), R v3.4.4 (2017), BEAST 2 (2014), BayesTraits v3 (2018).

Extended Data Legends

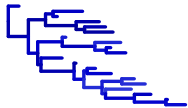
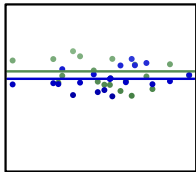
Extended Data Figure 1: Results of our N-1 jack-knife procedure for the mass (a) and wing area (b). Each point represents an individual species. We compare the imputed values for each species from our phylogenetic imputation procedure where that species has been excluded to the published value.

Extended Data Figure 2: Comparison of flight performance metrics between pterosaurs and extant bats and birds. In (a) we show the relationship between flight efficiency and mass in pterosaurs (as in Figure 2b, main text), with our mean phylogenetic imputations plotted with standard deviations shown by the green ellipses. We superimpose a previously reported relationship between flight efficiency and mass for extant birds (orange line), as well as data points for six bat species

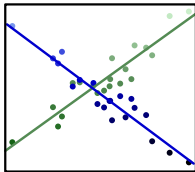
466 (blue crosses). In (b) is the relationship between sinking rate and mass for
467 pterosaurs (as in Figure 2c, main text), with our mean phylogenetic imputations
468 plotted with standard deviations shown by the blue ellipses. Superimposed, we show
469 the range of the relationship between sinking rate and mass for Procellariiformes
470 (orange box) and Accipitriformes⁷ (violet box) and individual data points for six
471 specimens of an extinct Cretaceous bird (*Sapeornis chaoyangensis*) (orange
472 quartered circles), 11 extant bird species (orange crosses), and seven bat species
473 (blue crosses). Triangles indicate pterosaur species for which we have published
474 data on mass, wing area, and wingspan. Circles indicate species for which we have
475 wingspan only. All azdarchoids are coloured in red.

a

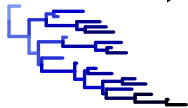
↑
efficiency (CoT^{-1})



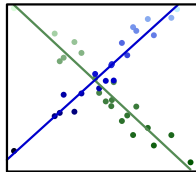
b



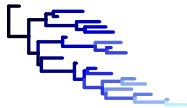
time (MY) →



c



↑
sinking rate (V_z)



a

